Activation of Pentamethylcyclopentadiene by Bk^+, Cf^+, and Es^+ Ions in the Gas Phase: Probing Electronic Structures of Transcurium Actinides

John K. Gibson* and Richard G. Haire

Chemical Sciences Division, Oak Ridge National Laboratory, Oak Ridge, Tennessee 37831-6375

Received August 6, 2004

Reactions of monopositive actinide ions, An^+, and lanthanide ions, Ln^+, with 1,2,3,4,5-pentamethylcyclopentadiene, HCp*, were studied by mass spectrometry. This was the first study of the M^+/HCp* reaction for $M^+ = Cm^+$, Cf^+, and Es^+; results for $M^+ = Am^+$, Bk^+, Pr^+, Eu^+, and Tm^+ are compared with those from previous studies. Different product distributions for the present experiments versus previous results for the same reactions are traced to a pressure effect whereby higher reactant pressures favor certain reaction channels. Each of the eight metal ions, M^+, reacted with HCp* to produce $[MCp^*]^+$ (+ H), as well as additional products. Both Cf^+ and Es^+ have previously been found to be inert toward most alkenes, but efficiently reacted with HCp* to induce (1) H-loss and $[AnCp^*]^+$; (2) H_2-loss and $[AnC_5(CH_3)_4(CH_2)]^+$; and (3) CH_3-loss and $[AnC_5(CH_3)_4H]^+$ (An = Cf, Es). These are the first organoeinsteinium complexes derived from activation of an organic substrate. The exhibited types of reactivity, i.e., product distributions, for the studied ions correlate with the energies to excite the ground-state atomic ions to configurations with two non-f valence electrons. It is concluded that the unidentified lowest-lying $[Rn]5f^{5}6d7s$ configuration of Cf^+ is ∼2.5 eV above the $[Rn]5f^{5}7s$ ground-state configuration. Secondary products included $[MCp^*_2]^+$ (M = Am, Cm, Bk, Cf, Es, Tm, and Pr), the compositions of which correspond to the metallocene sandwich complexes.

Introduction

Gas-phase reactions of actinide ions, An^+, with hydrocarbons have provided insights into fundamental aspects of molecular actinide chemistry.[1−7] A focus of recent studies has been systematic variations in reactivity related to metal ion electronic structures and energetics. It was concluded that the 5f electrons of the transneptunium An^+ cannot effectively participate in C−H or C−C bond activation.[7] Accordingly, transneptunium actinide ions exhibit reactivities that are indicative of lanthanide-like behavior. Here, the results of additional studies of reactions of Am^+, Cm^+, Bk^+, Cf^+, and Es^+ are reported. A particular emphasis is on the latter three transcurium ions in view of the difficulties encountered in examining their condensed phase organometallic chemistries and greater uncertainties in the atomic electronic energetics.

Previous studies of gas-phase reactions of Bk^+,[8] Cf^+,[9] and Es^+[10] with hydrocarbons focused on the activation of alkenes. The Bk^+ ion was found to exhibit significant reactivity only with easily activated cyclic alkenes: cyclooctatetraene (COT), cyclooctadiene, and 1,2,3,4,5-pentamethylcyclopentadiene (HCp*) where Cp* = *cyclo*-$C_5(CH_3)_5$, the electrophilic pentamethylcyclopentadienyl radical. In contrast to Pu^+, Bk^+ was inert toward other alkenes, such as butene.[6,8] Both Cf^+ and Es^+ were essentially inert toward activation of all of the studied alkenes.[9,10] Small yields of adducts such as $[Cf\text{-}COT]^+$ and $[Es\text{-butene}]^+$ were detected, but activation of C−H bonds (i.e., dehydrogenation) or C−C bonds (i.e., cracking) did not occur. These and results for reactions of other An^+ with hydrocarbons have been rationalized in the context of the electronic structures and energetics of the actinide ions.[7]

Activation of hydrocarbons by transition metal ions typically proceeds by an oxidative insertion mechanism that involves an intermediate in which the metal ion has been inserted into a covalent bond: $C-M^+-H$ or $C-M^+-C$.[11] These insertion mechanisms require two chemically active valence electrons at the metal center. Because the quasi-valence 4f electrons of the lanthanide

* Corresponding author. E-mail: gibsonjk@ornl.gov.

(1) Armentrout, P.; Hodges, R.; Beauchamp, J. L. *J. Am. Chem. Soc.* **1977**, *99*, 3162−3163.
(2) Armentrout, P. B.; Hodges, R. V.; Beauchamp, J. L. *J. Chem. Phys.* **1977**, *66*, 4683−4688.
(3) Heinemann, C.; Cornehl, H. H.; Schwarz, H. *J. Organomet. Chem.* **1995**, *501*, 201−209.
(4) Marçalo, J.; Leal, J. P.; Pires de Matos, A. *Int. J. Mass Spectrom. Ion Processes* **1996**, *157/158*, 265−274.
(5) Marçalo, J.; Leal, J. P.; Pires de Matos, A.; Marshall, A. *Organometallics* **1997**, *16*, 4581−4588.
(6) Gibson, J. K. *J. Am. Chem. Soc.* **1998** *120*, 2633−2640.
(7) Gibson, J. K. *Int. J. Mass Spectrom.* **2002**, *214*, 1−21.
(8) Gibson, J. K.; Haire, R. G. *Radiochim. Acta* **2001**, *89*, 709−719.
(9) Gibson, J. K.; Haire, R. G. *Int. J. Mass Spectrom.* **2000**, ***203***, 127−142.
(10) Gibson, J. K.; Haire, R. G. *Radiochim. Acta* **2003**, *91*, 441−448.
(11) Van Koppen, P. A. M.; Kemper, P. R.; Bowers, M. T. In *Organometallic Ion Chemistry*; Freiser, B. S., Ed.; Kluwer: Dordrecht, 1996; pp 157−196.

10.1021/om049387v CCC: $30.25
Publication on Web 11/30/2004

ions, Ln^+,[12−19] and 5f electrons of the transneptunium An^+ [7] have been shown to be chemically inert, the propensity of these f-element metal ions toward hydrocarbon activation generally correlates inversely with the promotion energy (PE) needed to excite the ion from its ground state to the lowest-lying electronic configuration with two spin-unpaired non-f valence electrons: the greater the PE, the lower the reactivity. The relationship between hydrocarbon activation and the ground-state electronic configurations and promotion energies for the Ln^+ has been examined by several groups.[12−19] The inert character of the 4f electrons and correlation between reactivities and promotion energies of the Ln^+ were studied in detail by Cornehl et al.[15] Armentrout and co-workers[20−23] have discussed the relationship between the electronic configurations of the first-row 3d transition metal ions and activation of hydrocarbons by oxidative insertion, as well as bonding in gas-phase organometallic complexes. There are intriguing analogies between the dependences on electronic structures found for the 3d transition elements[20−23] and those for the 4f lanthanides.[12−19]

The prepared divalent configurations are $[Xe]4f^{n-2}5d6s$ for most Ln^+[24] and $[Rn]5f^{n-2}6d7s$ for most An^+,[25,26] where "*n*" represents the total number of electrons outside the closed xenon and radon cores, respectively. An assessment of bonding in lanthanide and actinide oxides[27] has suggested a requirement for two valence d electrons at the metal center, i.e., $5d^2$ for the Ln^+ and $6d^2$ for the An^+, for formation of the M−O and M^+−O bonds. However, the correlation between PEs to the $[Xe]4f^{n-2}5d6s$ configurations and the reactivities of the Ln^+ [15] indicate that a "divalent" 5d6s, not $5d^2$, configuration is instead needed for hydrocarbon activation. The reactivities of An^+ with hydrocarbons[7] similarly indicate that it is the PE to the 6d7s, not $6d^2$, configuration that is pertinent. The PEs cited below correspond to PE[6d7s] for the An^+ and PE[5d6s] for the Ln^+.

Reactions with the HCp* substrate have been shown to be a useful probe of the electronic structures and energetics of lanthanide ions, Ln^+.[16,18] HCp* exhibits a high reaction efficiency with all Ln^+, even those such as Eu^+ (PE = 3.76 eV [24])[18] that are inert toward activation of other hydrocarbons.[15] The susceptibility of HCp* toward efficient bond activation by metal ions such as Sr^+,[18] which has only one valence electron, indicates reaction pathways that do not involve oxidative insertion. These proposed pathways are illustrated in Scheme 1. The C−CH_3 and C−H bonds at the saturated ring carbon of HCp* are sufficiently weak that cleavage can be induced by interaction of a metal ion with the π-electron system of the ring, resulting in the intermediates that are depicted by structures **2** and **3** in Scheme 1. Subsequent elimination of CH_3 or H results in the metal-tetramethylcylopentadienylide, $[MCp^\dagger]^+$ (product **4** in Scheme 1), or metal-pentamethylcyclopentadienylide, $[MCp^*]^+$, half-sandwich complex ions (product **5**), while elimination of H_2 results in the metal-tetramethylfulvene complex ion, $[MFv^\dagger]^+$ (product **6**).

Scheme 1

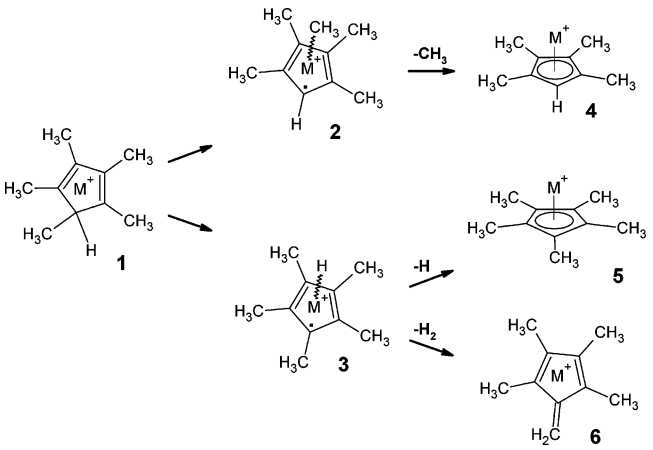

In our initial studies of the gas-phase organometallic chemistry of Cf^+ [9] and Es^+,[10] reactions with HCp* were not examined, and no significant activation was found with alkenes. In view of the special character of the HCp* substrate, we have now studied its reactions with Cf^+ and Es^+. Reactions of HCp* with Am^+, Cm^+, Bk^+, Pr^+, Eu^+, and Tm^+ were also examined to enable direct comparison with the results for Cf^+ and Es^+ under the same experimental conditions. This was the first study of the Cm^+/HCp*, Cf^+/HCp*, and Es^+/HCp* reactions. Several of the other M^+/HCp* reactions had been studied previously.[16,18,28] Among the motivations for this study were to probe the unknown energetics of the Cf^+ ion and to seek the first organoeinsteinium chemistry in which an organic substrate is activated. The HCp* reactant is of particular interest, not only because of its fragile nature but also because of the potential for formation of the archetypal $[MCp^*]^+$ "half-sandwich" (product **5** in Scheme 1) and $[Cp^*MCp^*]^+$ metallocene "sandwich" complexes.

Experimental Section

The experiments were performed using the laser ablation with prompt reaction and detection (LAPRD) technique employed previously in this laboratory to study actinide ion chemistry.[6−10,17,28] This methodology suffers limitations that are apparent from the presented results; notably, these results are largely qualitative and it is not possible to isolate specific

(12) Schilling, J. B.; Beauchamp, J. L. *J. Am. Chem. Soc.* **1988**, *110*, 15−24.
(13) Sunderlin, L. S.; Armentrout, P. B. *J. Am. Chem. Soc.* **1989**, *111*, 3845−3855.
(14) Yin, W. W.; Marshall, A. G.; Marçalo, J.; Pires de Matos, A. *J. Am. Chem. Soc.* **1994**, *116*, 8666−8672.
(15) Cornehl, H. H.; Heinemann, C.; Schröder, D.; Schwarz, H. *Organometallics* **1995**, *14*, 992−999.
(16) Marçalo, J.; Pires de Matos, A.; Evans, W. J. *Organometallics* **1996**, *15*, 345−349.
(17) Gibson, J. K. *J. Phys. Chem.* **1996**, *100*, 15688−15694.
(18) Marçalo, J.; Pires de Matos, A.; Evans, W. J. *Organometallics* **1997**, *16*, 3845−3850.
(19) Marçalo, J.; Pires de Matos, A. *J. Organomet. Chem*. **2002**, *647*, 216−224.
(20) Schultz, R. H.; Elkind, J. L.; Armentrout, P. B. *J. Am. Chem. Soc.* **1988**, *110*, 411−423.
(21) Armentrout, P. B.; Beauchamp, J. L. *Acc. Chem. Res.* **1989**, *22*, 315−321.
(22) Armentrout, P. B. *Science* **1991**, *251*, 175−179.
(23) Armentrout, P. B.; Kickel, B. L. In *Organometallic Ion Chemistry*; Freiser, B. S., Ed.; Kluwer: Dordrecht, 1996; pp 1−45.
(24) Martin, W. C.; Zalubas, R.; Hagan, L. *Atomic Energy Levels−The Rare-Earth Elements*; U.S. Department of Commerce: Washington, DC, 1978.
(25) Blaise, J.; Wyart, J.-F. *Energy Levels and Atomic Spectra of Actinides*; Tables Internationales de Constantes: Paris, 1992.
(26) Brewer, L. *J. Opt. Soc. Am.* **1971**, *61*, 1666−1682.
(27) Gibson, J. K. *J. Phys. Chem. A* **2003**, *107*, 7891−7899.
(28) Gibson, J. K. *Int. J. Mass Spectrom.* **2000**, *202*, 19−21.

reactant ions or interrogate product ions, as can be done using FTICR-MS.[18] The LAPRD approach has been employed here because of the restrictions imposed by handling the highly radioactive transcurium actinides. The LAPRD apparatus is enclosed in an alpha-containment glovebox such that there is minimal potential for the release of actinide materials into the laboratory. We know of no FTICR-MS configured to study highly radioactive nuclides such as ^{253}Es, which has a 21 day alpha-decay half-life. The details of the transuranium LAPRD instrument and procedures have been described elsewhere,[6,8−10,17,28] and only a brief synopsis of the experimental approach is included here.

The attenuated output from a XeCl excimer laser ($\lambda = 308$ nm) was focused (peak irradiance $\sim 10^8$ W cm^{-2}) onto the surface of a target pellet comprising one or more lanthanide and/or actinide oxide(s). Ablated ions propagated ~3 cm through the HCp* reagent (99.5%) injected into the reaction region via a leak valve and aiming tube. Because this approach employs nascent laser-ablated ions, it is important to note that it has been established that ground-state chemistry has been demonstrated for lanthanide and actinide ions, including those studied here, under these experimental conditions.[6−10,17] The HCp* pressure was monitored at a remote ion gauge, and the pressure in the reaction zone was indeterminate. The appearance of secondary products suggests multiple collisions, and pressure-dependent abundance distributions suggest a collisional cooling effect; these considerations are discussed below. After traversing the reaction zone, unreacted and product ions (and neutrals) entered the source region of a reflectron time-of-flight mass spectrometer and the positive ions were injected into the flight tube by a +200 V pulse applied to the ion repeller plate. The delay, t_d, between ion formation, i.e., the laser pulse, and ion sampling is variable. For short delay/reaction times (e.g., $t_d = 10$ μs), the product yield relative to unreacted ions was poor, and for long delay/reaction times (e.g., $t_d = 100$ μs), the sensitivity to the product ions was diminished. An intermediate delay, $t_d = 35$ μs, provided mass resolution of at least 1 amu and good sensitivity to product ions; most of the results were obtained using this delay. Longer delays were employed in some cases to obtain better mass resolution and/or to reduce the intensities of the most abundant product ions so that relative abundances could be determined. It was found that the relative abundances of activation products were essentially unchanged for delays between $t_d = 35$ μs and $t_d = 100$ μs. Mass spectra collected at 5 s^{-1} were averaged over 300 laser shots.

The ablation targets were copper disks containing a few atomic percent of one or more actinide and/or lanthanide sesquioxide, M_2O_3.[6,8−10] The targets were prepared by physically mixing the constituent powders and compacting the mixture in a pellet press. The following six targets were employed in this work: *Es*/*Eu*/*Tm*; *Bk*/*Es*/*Eu*/*Tm*; *Tm*/*Pr*; *Am*; *Cm*; and *Cf*. The *Es*/*Eu*/*Tm* target was prepared using 190 μg of ^{253}Es, ~3% of which had decayed to the ^{249}Bk daughter at the time of the experiments; comparable amounts of natural Eu and Tm were included in this multicomponent target. The alpha-decay half-life of ^{253}Es is 20.5 days so that 22 days after preparation of the *Es*/*Eu*/*Tm* target the resulting *Bk*/*Es*/*Eu*/*Tm* contained approximately equal amounts of remaining ^{253}Es and its decay product, ^{249}Bk. The beta-decay half-life of ^{249}Bk is 320 days so that the concentration of the ^{249}Cf granddaughter of ^{253}Es in the *Bk*/*Es*/*Eu*/*Tm* target was minimal. The main ions ablated from the M_2O_3 were M^+ and MO^+. For Pr_2O_3, PrO^+ was dominant and only a small amount of bare Pr^+ was ablated. For Cm_2O_3 and Bk_2O_3, the yields of the bare M^+ and MO^+ were comparable. For the other M_2O_3 (M = Am, Cf, Es, Eu, Tm), bare M^+ was dominant. The MO^+ abundances correlate with the M^+-O bond energies.[6,8−10]

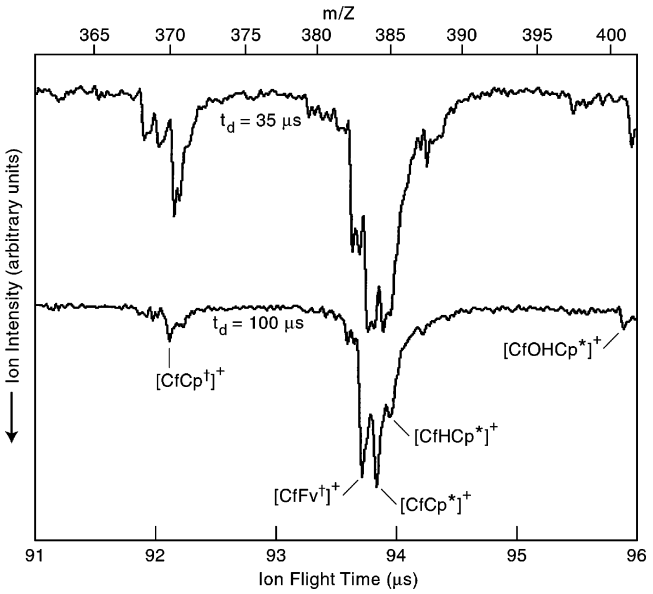

Figure 1. Primary product ion mass spectra for the reaction of Cf^+ with HCp*. The top spectrum is for an ablation-to-detection delay (t_d) of 35 μs and the bottom spectrum for a delay of 100 μs. The minor $[CfOHCp^*]^+$ association product ($m/z = 401$) resulted from the reaction of a small amount of ablated CfO^+.

Results and Discussion

The dominant primary reactions of bare M^+ that were observed in the present work are given by eqs 1−4 (n = 1, 2 in eq 4).

$$M^+ + C_5(CH_3)_5H \rightarrow [MC_5(CH_3)_4H]^+ + CH_3 \quad (1)$$

$$\rightarrow [MC_5(CH_3)_5]^+ + H \quad (2)$$

$$\rightarrow [MC_5(CH_3)_4CH_2]^+ + H_2 \quad (3)$$

$$\rightarrow [MC_5(CH_3)_{4-2n}(CH_2)_{2n+1}]^+ + (n+1)H_2 \quad (4)$$

Referring to Scheme 1, eq 1 corresponds to the sequence **1** → **2** → **4**, eq 2 to **1** → **3** → **5**, and eq 3 to **1** → **3** → **6**. Not all four types of reaction were exhibited by each metal ion.

Portions of representative product mass spectra are shown in Figure 1 for the reaction of Cf^+ and CfO^+ with HCp*. The top spectrum corresponds to an ablation-to-detection delay, t_d, of 35 μs and the bottom spectrum to a delay of 100 μs. The sensitivity to reaction products is greater for the shorter delay, whereas the mass resolution is better for the longer delay. The mass scale shown at the top of the figure corresponds to the higher-resolution $t_d = 100$ μs spectrum. The apparent shift to higher masses, i.e., longer ion flight times, for the short-delay spectrum is taken to primarily reflect peak tailing due to detector saturation. The longer delay spectrum also shows clearly that the abundances of the two major products were nearly the same. The greater sensitivity for short delays allows identification of minor products, such as those at m/z 368 and 369 that correspond to additional H-loss from $[CfCp^\dagger]^+$.

Pressure-Dependence of Product Distributions. In an earlier study, reactions of Np^+, Pu^+, and Am^+ with

HCp* were studied using the LAPRD technique.[28] The dominant product for Am^+ in that study was **6**, $[AmFv^\dagger]^+$, corresponding to eq 3. Product **5**, $[AmCp^*]^+$, i.e., eq 2, was not observed. In the present study, both $[AmFv^\dagger]^+$ and $[AmCp^*]^+$ were produced in comparable yields. The main difference between the two LAPRD experiments was that the HCp* pressure was about an order of magnitude higher for the present studies, to enhance sensitivity to low-abundance products.

To evaluate effects of reagent pressure on product distributions, reactions of Am^+ with HCp* were carried out under different HCp* pressures. The "low-pressure" experiments corresponded to a gauge reading of 2×10^{-6} Torr HCp* and the "high-pressure" experiments to 5×10^{-5} Torr HCp*, the latter being the approximate reagent pressure used for the other experiments discussed in the following sections. Under the low-pressure conditions the dominant product was **6**, $[AmFv^\dagger]^+$; the abundance of **5**, $[AmCp^*]^+$, was comparatively negligible. Under the high-pressure conditions the abundances of **5** and **6** were essentially the same. The low-pressure product distribution (i.e., relative abundance **6** ≫ **5**) is in good agreement with the previous LAPRD results under similar conditions.[28] Under both reagent pressure conditions, some product **4**, $[AmCp^\dagger]^+$, was also produced.

Under the low-pressure conditions the dominant reaction pathway is **1** → **3** → **6**, with H_2-elimination predominating. Upon increasing the reagent pressure by a factor of ~25×, pathways **1** → **3** → **5** and **1** → **3** → **6**, i.e., eqs 2 and 3, become approximately equally probable. At least one secondary product was detected under both the low-pressure and high-pressure conditions. At low pressures, a small amount of $[AmCp^*_2]^+$ was produced. At the higher pressure, the yield of $[AmCp^*_2]^+$ increased by more than an order of magnitude, and lesser amounts of $[AmCp^*Cp^\dagger]^+$, $[AmCp^*Fv^\dagger]^+$, and $[AmFv^\dagger_2]^+$ also appeared. The increase in yields of secondary products under the higher-pressure conditions indicates a greater probability for collisions of primary products with additional HCp* molecules. The conclusion is that the dominant reaction pathway for intermediate **3** (M = Am), absent collision with a second HCp* molecule, is elimination of H_2 to yield product **6**. Collision of intermediate **3** with a second HCp* molecule may enhance the H-loss channel, or perhaps nascent product **5** is susceptible to fragmentation absent collisional cooling.

In a quadrupole ion trap mass spectrometry study of reactions of Ln^+ with HCp*,[29] it was found that the pressure of the neon bath gas influenced the product distributions. It was concluded that collisional cooling under the higher-pressure conditions (4×10^{-4} Torr Ne) resulted in energy dissipation from internally "hot" nascent intermediates and/or products, thereby enhancing certain reaction pathways.[29] In the QIT study, the yield of the H-loss product **5** was enhanced relative to that of product **6** when compared with results under low-pressure FTICR-MS conditions,[16,18] consistent with the present results.

The reaction of Bk^+ with HCp* was previously studied by the LAPRD method at relatively low pressures[8] with the only significant products being $[BkFv^\dagger]^+$ and $[Bk(HCp^*\text{-}2H_2)]^+$, corresponding to eqs 3 and 4 ($n = 1$). In the present work, the dominant product was again $[BkFv^\dagger]^+$, but lesser amounts of $[BkCp^*]^+$, $[Bk(HCp^*\text{-}2H_2)]^+$, and $[Bk(HCp^*\text{-}3H_2)]^+$ were also produced, according to eqs 2 and 4 ($n = 1, 2$). This suggests that **1** → **3** → **5** is a significant pathway for M = Bk upon collisional cooling of the intermediate and/or product.

Table 1. Main Products for the M^+/HCp* Reactions, $[MHCp^*\text{-}E]^+$[a]

	E
Am^+	$H \approx H_2 > CH_3$
Cm^+	$H_2 > H \approx 3H_2$
Bk^+	$H_2 > H \approx 3H_2$
Cf^+	$H \approx H_2 > CH_3$
Es^+	$H > H_2 > CH_3$
Pr^+	$H_2 > 3H_2 > 2H_2$
Eu^+	$H > CH_3 > H_2$
Tm^+	$H \approx H_2 > CH_3$

[a] Only the three main products for each reactant ion are included. The products are identified by the radicals and molecules, E, eliminated from the HCp* reactant molecule: E = CH_3 corresponds to **4** ($[MCp^\dagger]^+$) in Scheme 1, E = H to **5** ($[MCp^*]^+$), and E = H_2 to **6** ($[MFv^\dagger]^+$). The relative product abundances are indicated qualitatively. The potential for a contribution to the E = H_2 channel from the MO^+/HCp* reactions (M = Pr, Cm, Bk) is discussed in the text. The three main product ion peaks for the Cf^+/HCp* reaction are identified in Figure 1.

In view of the demonstrated dependence of the LAPRD results on the reagent pressure, the present series of comparative experiments were carried out under similar conditions. Specifically, the uncorrected HCp* pressure measured at the remote ion gauge was in the relatively narrow range of $(4-9) \times 10^{-5}$ Torr. If a relative gauge sensitivity of ~10 for HCp* is employed,[29] this corresponds to $(4-9) \times 10^{-6}$ Torr HCp*. Experiments carried out with Cm^+ revealed only minor changes in product distributions in this pressure range. It is not practical to infer the reagent pressure in the reaction zone from the measurement at the remote ion gauge, but it can be conservatively estimated that it was at least an order of magnitude greater: $P_{rxn}[HCp^*] \geq 10^{-4}$ Torr. It is expected that different product distributions would be found for the studied reactions under single-collision conditions, such as are encountered in FTICR-MS.[16,18]

Products of Reactions with HCp*: Hydrocarbon Activation by Cf^+ and Es^+. It has been reported[18] that the reactions of all of the Ln^+ with HCp* are rather efficient, typically proceeding at approximately half the collision rate. Results for An^+ [28] have indicated a similarly high reactivity. The product yields in the present study were typically ~10% relative to unreacted ions, this being consistent with a reagent pressure somewhat greater than 1×10^{-4} Torr, as estimated above. The product yields for the M^+/HCp* reactions were particularly small when the amount of reactant M^+ was small due to a low concentration of M_2O_3 in the target and/or prevalence of the ablated monoxide ion, MO^+. Because of the resulting limited sensitivity to reaction products, only the three most prominent products are reported for each reactant metal ion. The results are presented in Table 1, where the relative yields for the three dominant primary products for each M^+/HCp* reaction are given in order of abundance. The absolute M^+/HCp* reaction rates were not measured,

(29) Jackson, G. P.; Gibson, J. K.; Duckworth, D. C. *Int. J. Mass Spectrom.* **2002**, *220*, 419−441.

but substantial reactivity was exhibited for each metal ion, in accord with the FTICR-MS results.[16,18]

Gas-phase reactions of each of the studied metal ions with alkenes other than HCp* have been examined previously.[7−10,15] The Cf^+ ion was unreactive with propene, butene, cyclohexadiene, cyclohexene, and cycooctatetraene (COT).[9] The only significant Cf^+/alkene reaction product was the $[Cf\text{-}COT]^+$ adduct. Similarly, Es^+ was inert toward butene, cyclooctadiene, 1-methyl-1-cyclohexene, and benzene.[10] The only alkene reaction product detected for Es^+ was the adduct, $[Es\text{-butene}]^+$. In the previous studies with Cf^+ and Es^+, the fragile HCp* substrate was not included as a reagent. The products **4**, **5**, and **6** for M = Cf and Es thus represent the first examples of hydrocarbon activation by Cf^+ and Es^+. The crystalline californium tris-cyclopentadienyl organometallic compound, $Cf(C_5H_5)_3$, i.e., the unsubstituted $CfCp_3$ analogue of hypothetical $CfCp^*_3$, has been prepared by the metathesis reaction of $CfCl_3$ with molten $Be(C_5H_5)_2$.[30] The scarcity and high specific activity of available Es isotopes have precluded the isolation of any organoeinsteinium compounds.[31] The three reactions shown in Scheme 1 for M = Cf and Es represent the first preparation of organocalifornium and organoeinsteinium complexes by activation of an organic substrate.

Product Distributions: Two Types of M^+ Reactivity. Two basic types of reactivity are exhibited, as indicated by the product distributions in Table 1. For Am^+, Cf^+, Es^+, Eu^+, and Tm^+ the three dominant reaction channels are elimination of H, H_2, and CH_3 (i.e., eqs 1−3 and Scheme 1; the results for Cf^+ are shown in Figure 1); these are referred to as type ***D*** (i.e., direct) metal ions. For Cm^+, Bk^+, and Pr^+ the dominant reaction channels include elimination of more than one H_2 molecule (i.e., eq 4); these are referred to as type ***I*** (i.e., insertion) metal ions. The reactivity pattern of the type ***D*** ions is characteristic of the noninsertion, so-called "direct",[16,18] mechanism shown in Scheme 1. The appearance of channels corresponding to the elimination of two or three H_2 molecules for the type ***I*** ions indicates reaction mechanisms that involve oxidative insertion of the metal ion into C−H bonds to produce $C\text{−}M^+\text{−}H$ types of intermediates.[16,18]

As has been shown in previous studies of reactions of An^+ and Ln^+ ions with HCp*, the product distributions vary depending on the electronic structure and energetics of the reacting f-element ion.[16,18,28] Specifically, there is a distinct relationship between the types of reactivities and the PEs to excite the ground-state ion to an electronic configuration with two spin-unpaired non-f valence electrons. This relationship is attributed to the inert character of the quasi-valence f electrons and the need for two chemically active valence electrons at the metal center for bond activation via an oxidative insertion mechanism. For An^+ and Ln^+ with large PEs (i.e, greater than ∼2 eV),[24,25] the HCp* substrate is activated, absent oxidative insertion, via the mechanisms shown in Scheme 1, to produce $[MCp^\dagger]^+$ (CH_3-elimination), $[MCp^*]^+$ (H-elimination), and $[MFv^\dagger]^+$ (H_2-elimination).[18,28] The metal ions that exhibit this type of reactivity are precisely those that are nearly inert toward most other alkenes.[7,15] For An^+ and Ln^+ with small PEs (i.e., less than ∼1.6 eV,[24,25] the dominant reaction pathways include those that require oxidative insertion; products corresponding to multiple H_2-elimination are prominent.[18,28] The PEs for excitation from the ground states to the 6d7s and 5d6s "divalent" configurations are included in Table 2. For most alkenes, the magnitude of the PE to a prepared divalent state determines the relative reaction efficiency, but in the distinctive case of HCp* it is the product distribution, not the reaction efficiency, that varies with the PEs. This dependence is employed below to estimate relative PEs of characteristically unreactive (i.e., large PE) metal ions.

Table 2. Promotion Energies and Dehydrogenation Product Distributions

	Am^+	Cm^+	Bk^+	Cf^+	Es^+	Pr^+	Eu^+	Tm^+
PE (eV)[a]	2.55	0.50	1.53	(3.00)[b]	2.85 ± 0.25	0.98	3.76	2.06
$A[MCp^*]^+$ [c]	1	0.4	0.2	1	1	0.2	1	1
$A[MFv^\dagger]^+$ [c]	1	1[d]	1[d]	1	0.3	1[d]	0.3	1
reactivity type[e]	***D-1***	***I***	***I***	***D-1***	***D-2***	***I***	***D-2***	***D-1***

[a] Promotion energies (PEs) to excite the free ion from its ground state to the lowest lying $[Rn]5f^{n-2}6d7s$ (for An^+) or $[Xe]4f^{n-2}5d6s$ (for Ln^+) configuration. The values for the An^+ are from Blaise and Wyart;[25] those for the Ln^+ are from Martin et al.[24] [b] The PE for Cf^+ from Blaise and Wyart[25] may not be the lowest-lying configuration. Brewer[26] has estimated a lower value of 2.54 ± 0.37 eV. [c] Cp* represents the pentamethylcyclopentadienyl radical, $C_5(CH_3)_5$, and corresponds to H-elimination from HCp*. $Fv^\dagger$ represents the tetramethylfulvene ligand, $C_5(CH_3)_4CH_2$, and corresponds to H_2-elimination from HCp*. The abundance, A, of the major product is defined as 1; the comparative fractional abundances of the minor products are considered uncertain by approximately ±0.2 due to variations between experiments and the peak overlap for these products, which are separated in mass by 1 amu. [d] The potential for some contribution to $A[MFv^\dagger]^+$ from the MO^+/HCp* reactions (M = Pr, Cm, Bk) is discussed in the text. [e] The three reactivity types, ***I*** (insertion), ***D-1*** (direct type 1), and ***D-2*** (direct type 2), are discussed in the text.

The results in Table 1 along with the PEs in Table 2 reveal a correlation between the reactivity and promotion energy of a metal ion. The metal ions that exhibit reactivity type ***D***, denoted as ***D-1*** and ***D-2*** in Table 2, all exhibit a $PE[M^+]$ of 2.06 eV (i.e., $PE[Tm^+]$) or greater, whereas those that exhibit reactivity type ***I*** have a $PE[M^+]$ of 1.53 eV (i.e., $PE[Bk^+]$) or less. This result appeared in a FTICR-MS study of reactions of Ln^+ ions with HCp*,[18] where reaction channels that required oxidative insertion (type ***I***) appeared only when $PE[Ln^+] \leq 1.46$ eV (i.e., $PE[Lu^+]$). For Tm^+ ($PE[Tm^+] = 2.06$ eV[20]) and lanthanide ions exhibiting larger $PE[Ln^+]$, i.e., Sm^+, Eu^+, and Yb^+, the observed reaction pathways were attributed to the direct type of mechanisms[18] depicted in Scheme 1.

The present results obtained under relatively high HCp* pressures are consistent with two essential types of reactivity, as determined by the ability of the metal ion to oxidatively insert into C−H and/or C−C bonds. For those M^+ with prohibitively large PEs, the three products given in Scheme 1 were observed, albeit with different relative abundances than were found under low-pressure conditions. For the three M^+ (Cm^+, Bk^+, Pr^+) with sufficiently small PEs that insertion mechanisms are allowed, H_2-elimination was the dominant reaction pathway; however, some H-elimination product **5**, $[MCp^*]^+$, as well as multiple H_2-elimination, was also

(30) Laubereau, P. G.; Burns, J. H. *Inorg. Chem.* **1970**, *9*, 1091−1095.
(31) Hulet, E. K. In *The Chemistry of the Actinide Elements*, 2nd ed.; Katz, J. J., Seaborg, G. T., Morss, L. R., Eds.; Chapman and Hall: New York, 1986; pp 1071−1084.

observed for the type ***I*** metal ions. In contrast, neither $[BkCp^*]^+$ [8] nor $[PrCp^*]^+$ [18] was previously identified from the corresponding M^+/HCp^* reaction under low-pressure conditions. The Cm^+/HCp^* reaction to give $[CmCp^*]^+$ and other products was not studied previously. The appearance of these three $[MCp^*]^+$ (M = Cm, Bk, Pr) suggests that the reaction pathway **1** → **3** → **5** occurs for An^+ and Ln^+ with small PEs under high-pressure conditions where reaction pathways are influenced by third-body collisions of intermediates and/or products with additional HCp* molecules. Although the type ***I*** group of M^+ with relatively small PEs (e.g., Cm^+, Bk^+, Pr^+) can activate HCp* by oxidative insertion, the direct mechanism (i.e., Scheme 1) should also be accessible. That the $[MCp^*]^+$ product was not previously observed for type ***I*** ions[18,28] suggests that the reaction sequence **1** → **3** → **5** was not competitive under those experimental conditions. In accord with the enhancement in this otherwise minor channel for type ***D*** ions under the high-pressure HCp* conditions employed in the present work, this mechanism was also evidently enhanced for type ***I*** ions, to the extent that $[MCp^*]^+$ was a significant product for both types of An^+ and Ln^+, ***I*** and ***D***. The generally greater yields of products **5** and/or **6** compared with **4** suggest that the initial interaction of a metal ion with HCp* results primarily in intermediate **3** rather than **2**; that is, C−H bond cleavage at the saturated ring carbon is evidently favored over C−C bond cleavage.

Reactions of MO^+ and Secondary Reactions of M^+. All of the lanthanide monoxide ions, LnO^+, are known to react efficiently with HCp* ($k/k_{ADO} \geq 0.5$).[18] The observed variations in product distributions are related to the Ln^+-O bond strengths.[18] Because the amounts of ablated MO^+ are directly related to the widely ranging M^+-O bond energies, the MO^+ abundances are widely variable and it is not possible to systematically study their chemistry using the LAPRD technique. From the *Pr*/*Tm* target, for example, the amount of ablated PrO^+ was ∼20× that of bare Pr^+, whereas the amount of ablated bare Tm^+ was ∼20× that of TmO^+. These very disparate oxide abundances reflect the Pr^+-O and Tm^+-O bond energies, 792 and 478 kJ mol^{-1}, respectively.[32] In accord with the FTICR-MS results,[18] a major product of the reaction of the abundant PrO^+ with HCp* was the association product, $[PrOHCp^*]^+$. Formulation of the association complex as the hydroxide pentamethylcyclopentadienylide, $[(Cp^*)Pr(OH)]^+$, has not been experimentally confirmed.[16,18] An alternative formulation is the simple adduct $[OPr(HCp^*)]^+$. In the present study, the association product was identified for M = Am, Cm, Bk, Cf, Pr, and Tm (the $[CfOHCp^*]^+$ peak is identified in Figure 1). Insufficient EsO^+ and EuO^+ were available to effectively study their chemistries. The FTICR-MS study of the TmO^+/HCp^* reaction[18] indicated that $[TmOFv^\dagger]^+$ (+ H_2) was the main pathway (66% abundance), and $[TmOHCp^*]^+$ was relatively minor (15%). In contrast, under the higher-pressure LAPRD conditions, the abundance of $[TmOHCp^*]^+$ was substantially greater than that of $[TmOFv^\dagger]^+$. In analogy with the interpretation of the results for the bare metal ion, it is postulated that collisions with additional HCp* molecules stabilize the association complex against fragmentation.

Secondary products from the reaction of a bare metal ion and/or a metal oxide ion with two HCp* molecules were identified for most of the studied metals. In each case where one or more secondary products were identified, the major such species was $[MCp^*_2]^+$; this was identified for M = Am, Cm, Bk, Cf, Es, Tm, and Pr. This product might initially be presumed to comprise the $\{(H_3C)_5C_5\}$-η^5-M-η^5-$\{C_5(CH_3)_5\}$ metallocene structural component that is prevalent in organoactinide and organolanthanide chemistry.[33,34] Marçalo et al.[16] examined the pathway to $SmCp^*_2{}^+$ from the Sm^+/HCp^* reaction and determined that the formation of this product occurs via the tetramethylfulvene primary product **6**, $[SmFv^\dagger]^+$. Addition of a second HCp* to $[MFv^\dagger]^+$ gives a product with composition formally corresponding to $[MCp^*_2]^+$ according to eq 5, where the suggested structural formulation has not been established.

$$[MFv^\dagger]^+ + HCp^* \rightarrow [MCp^*_2]^+ \qquad (5)$$

Although, it is impractical to directly identify the origins of these secondary products using the LAPRD technique, the present results are qualitatively consistent with the availability of this same pathway to the $[MCp^*_2]^+$ identified here. Specifically, the yields of $[MCp^*_2]^+$ were found to correlate with those of $[MFv^\dagger]^+$. The very small yield of $[EsCp^*_2]^+$, as well as the inability to confidently detect $[EuCp^*_2]^+$, is attributed to the atypically small amounts of the $[MFv^\dagger]^+$ precursor for these two metal ions.

The identification of $[EsCp^*_2]^+$ is particularly noteworthy in view of the unknown nature of organoeinsteinium chemistry. This might be presumed to be the bis-cyclopentadienylide metallocene in which the Es metal center is in a formally trivalent oxidation state: $[Cp^*$-η^5-Es(III)-η^5-$Cp^*]^+$. It should be noted that the $[MFv^\dagger]^+/HCp^*$ reaction was previously reported to result in compositions corresponding to $[MCp^*_2]^+$ for M = Ca, Sr, and Ba,[18] for which the trivalent oxidation state is inaccessible. In view of the formation of the product formally corresponding to $[MCp^*_2]^+$ for alkaline earth metals, the alternative structural formulation, $[(HCp^*)MFv^\dagger]^+$, was proposed.[18] However, the bonding in $[Cp^*MCp^*]^+$ (M = Ca, Sr, Ba) may be primarily electrostatic and the stability of these species could be enhanced by the small second ionization energies: 11.87 eV for Ca^+;[35] 11.03 eV for Sr^+;[36] and only 10.00 eV for Ba^+.[37]

Product Distributions: Comparative Promotion Energies. As discussed above, two basic types of reactivity were observed, type ***I*** (Cm^+, Bk^+, Pr^+) and type ***D*** (Am^+, Cf^+, Es^+, Eu^+, Tm^+), where the observed reaction pathways are related to the PEs to achieve a

(32) Chandrasekharaiah, M. S.; Gingerich, K. A. In *Handbook on the Physics and Chemistry of Rare Earths*, *Vol. 12*; Gschneidner, K. A., Jr., Eyring, L., Eds.; Elsevier: Amsterdam, 1989; pp 409−431.

(33) Evans, W. J., Davis, B. L. *Chem. Rev.* **2002**, *102*, 2119−2136.

(34) Evans, W. J. *J. Organomet. Chem.* **2002**, *647*, 2−11.

(35) Martin, W. C.; Sugar, J.; Musgrove, A. *NIST Atomic Spectra Database (NIST Standard Reference Database #78)*; U.S. Department of Commerce: Washington, DC, 2004 (http://physics.nist.gov/cgi-bin/AtData/main_asd).

(36) Moore, C. E. *Atomic Energy Levels*, *Vol. II (NBS Circular 467)*; U.S. Department of Commerce: Washington, DC, 1952.

(37) Moore, C. E. *Atomic Energy Levels*, *Vol. III (NBS Circular 467)*; U.S. Department of Commerce: Washington, DC, 1958.

prepared divalent bonding state of the metal ion. Further examination of the product distributions suggests that the type ***D*** metal ions exhibit two reactivity subtypes, ***D-1*** and ***D-2***, as reflected in the relative abundances of the H-loss product, $[MCp^*]^+$, and the H_2-loss product, $[MFv^\dagger]^+$. As indicated in Table 1, the abundances of these two products are approximately comparable for Am^+, Cf^+, and Tm^+ (the results for Cf^+ are shown in Figure 1); this is denoted as reactivity type ***D-1***. In contrast, for Es^+ and Eu^+ it was evident that the H-loss product was substantially more abundant than was the H_2-loss product; this is denoted as reactivity type ***D-2***. Approximate values for the relative abundances of these two products for each of the studied M^+ are given in Table 2, along with the metal ion PEs. For the type ***D*** metal ions, there would appear to be a correlation between the PEs and the reactivity subtype: $A[MCp^*]^+ \approx A[MFv^\dagger]^+$ for $PE \leq PE[Cf^+]$ (type ***D-1***) and $A[MCp^*]^+ > A[MFv^\dagger]^+$ for $PE \geq PE[Es^+]$ (type ***D-2***). The type of reactivity that has been attributed to each studied metal ion is indicated in Table 2.

A drawback of the LAPRD approach is the inability to identify the specific precursor reactant ion when more than one pathway to a particular product is feasible. In addition to its formation via H_2-elimination in the M^+/HCp* reaction, the $[MFv^\dagger]^+$ product can be accessed by H_2O-elimination in the MO^+/HCp* reaction,[16,18] eq 6.

$$MO^+ + HCp^* \rightarrow [MFv^\dagger]^+ + H_2O \qquad (6)$$

However, the contribution from this reaction may have been significant only for the type ***I*** ions, for which substantial amounts of the oxide ion were ablated: CmO^+, BkO^+, and PrO^+. Because Cm^+, Bk^+, and Pr^+ exhibited the same distinctive type ***I*** reactivity pattern, a contribution to the $[MFv^\dagger]^+$ abundance from dehydration of their MO^+ does not complicate interpretation of the results for the type ***D*** ions.

Although the higher pressures of the LAPRD experiments result in very different product distributions compared with the low-pressure FTICR-MS studies,[18] the two basic types of reactivity, ***I*** and ***D***, are reflected in the relative product distributions under both experimental conditions. The FTICR-MS results can furthermore be assessed in the context of the reactivity subtypes that are postulated here for the type ***D*** ions, these being Sm^+, Eu^+, Tm^+, and Yb^+ in the lanthanide series. Using the results from Table 1 of ref 18, the following relative abundance ratios, $R[Ln^+] \equiv \{A[LnCp^*]^+/A[LnFv^\dagger]^+\}$ are obtained: $\{R[Eu^+] = 0.33\} > \{R[Yb^+] = 0.10\} \geq \{R[Sm^+] = 0.09\} > \{R[Tm^+] = 0.02\}$. The corresponding $PE[Ln^+]$ are as follows:[24] $\{PE[Eu^+] = 3.76\ eV\} > \{PE[Yb^+] = 3.32\ eV\} > \{PE[Sm^+] = 2.68\ eV\} > \{PE[Tm^+] = 2.06\ eV\}$. The earlier FTICR-MS results are consistent with the two postulated reactivity subtypes, ***D-1*** and ***D-2***. The abundance ratios for the alkaline earth ions studied by FTICR-MS[18] are excluded from this assessment because these ions have only one valence electron outside of the rare gas core so that $PE[M^+]$ to a divalent configuration is not relevant. The large variations in reactivity within the alkaline earth group[18] can instead be attributed to differences in properties such as ionic radii, second ionization energies (IEs), and electronic polarizabilities. Among the alkaline earths, Ba^+ ($Z = 56$) should behave most similarly to the Ln^+ ($Z = 57-71$). The FTICR-MS results—$\{A[BaCp^*]^+/A[BaFv^\dagger]^+\} = 0.94$[18]—suggest that the abundances of the two products would be comparable for a lanthanide ion with an extremely large "PE" (e.g., $PE > IE[Ba^+] = 10.00$ eV).[37]

Based on the present LAPRD results and the earlier FTICR-MS results,[18] it is concluded that for the actinide and lanthanide ions the dissociation reaction pathway **3** → **6** is enhanced by the accessibility of a second valence electron at the metal center. Furthermore, we propose that pathways **3** → **6** and **3** → **5** should become approximately equally probable under collisonless conditions for a lanthanide-like monopositive metal ion (i.e., Ba^+) when a second valence electron at the metal center is not available. It is reasonable to postulate that pathway **3** → **6** proceeds in a facile manner by abstraction of an H atom from a methyl group via a species that can be represented as $\{Fv^\dagger\}$-$\{H-M^+-H\}$. This dihydrido intermediate formally requires two (non-f) valence electrons at the metal center and should become less viable as $PE[M^+]$ increases. However, the observation[18] that even monovalent ions such as Ba^+ induce H_2-elimination indicates that the requirement for formation of two fully covalent bonds is not rigorous. In contrast to pathway **3** → **6**, pathway **3** → **5** should proceed by straightforward elimination of the H atom; the efficiency of this process would then be unaffected by the accessibility of a second bonding valence electron at the metal center. This mechanistic picture is consistent with the trend of increasing $\{A[MCp^*]^+/A[MFv^\dagger]^+\}$ with increasing $PE[M^+]$.

The preceding assessment of the abundance distributions permits using the An^+/HCp* results to estimate unknown PEs. As indicated in Table 2, $PE[Es^+] = 2.85 \pm 0.25$ eV.[25] It has been noted by Blaise and Wyart[25] that the spectroscopically determined $PE[Cf^+] = 3.00$ eV may not correspond to the lowest-lying $[Rn]5f^56d7s$ configuration.[25] Brewer[26] has estimated a smaller $PE[Cf^+] = 2.54 \pm 0.37$ eV. The relative abundances of $[MCp^*]^+$ and $[MFv^\dagger]^+$ (Table 2) would imply that $PE[Es^+] > PE[Cf^+]$ and $PE[Es^+] > PE[Am^+]$. These relationships suggest that the assigned $[Rn]5f^56d7s$ level for Cf^+ at 3.00 eV above ground[25] indeed is not the lowest-lying such level. Instead, Brewer's estimate,[26] $PE[Cf^+] = 2.54 \pm 0.37$ eV, is consistent with the experimental observations and inference therefrom that $PE[Cf^+] < PE[Es^+] = 2.85 \pm 0.25$ eV. The conclusion is that $PE[Cf^+] \approx PE[Am^+] = 2.55$ eV.[25]

Conclusions

Gas-phase reactions of the first five transplutonium An^+, as well as selected Ln^+, were studied. This represents the first examination of the An^+/HCp* reactions for $An^+ = Cm^+$, Cf^+, and Es^+. The HCp* reaction substrate is of particular interest because of its susceptibility to fragmentation induced by metal ions that are inert toward most organic molecules;[18] such inert character is seen for Cf^+ [9] and Es^+.[10] The origins of substantial discrepancies between product distributions from the present work and those determined previously for An^+ and Ln^+ ions[18,28] were explored for Am^+. The higher-pressure conditions of the present studies particularly favored the H-elimination channel, thereby enhancing the production of $[MCp^*]^+$ relative to $[MFv^\dagger]^+$.

Two types of metal ion reactivity were manifested, as had been found previously for Ln^+,[18] as well as some An^+.[28] This behavior has now been demonstrated for Cm^+, Cf^+, and Es^+. The "direct" type of reactivity requires only one non-f valence electron at the metal ion center and is characteristic of those f element M^+ that require energies in excess of ~2 eV to achieve an excited-state configuration with two non-f valence electrons. Of the metal ions studied here, the direct type of reactivity was exhibited by Am^+, Cf^+, Es^+, Eu^+, and Tm^+. The main products of direct reaction mechanisms are $[MCp^*]^+$ (i.e., H-loss), $[MFv^\dagger]^+$ (i.e., H_2-loss), and $[MCp^\dagger]^+$ (i.e., CH_3-loss). For M = Cf and Es, these are the first examples of activation of an organic substrate; only the metathesis product, the californium tris-cyclopentadienylide compound, has been isolated.[30] The alternative "insertion" type of reactivity is exhibited by those metal ions that have divalent configurations within ~1.6 eV of the ground state and that can therefore activate C−H (and C−C) bonds by oxidative insertion. Multiple H_2-elimination is a characteristic reaction pathway for these metal ions; the type ***I*** ions in the present study were Cm^+, Bk^+, and Pr^+. Secondary products corresponding to the formulation $[MCp^*_2]^+$ were identified for M = Am, Cm, Bk, Cf, Es, Pr, and Tm.

For the metal ions that exhibit "direct" reaction mechanisms, there is convincing correlation between the magnitude of the promotion energy to achieve a divalent bonding configuration and the relative contributions of the H-loss and H_2-loss channels. On the basis of the relationship between promotion energies and the comparative extents of H-loss and H_2-loss, it is inferred that $PE[Es^+] > PE[Cf^+]$ and concluded that the spectroscopically determined PE to the excited state $[Rn]5f^5 6d7s$ configuration for Cf^+, at 3.00 eV above ground,[25] is not the lowest-lying such configuration. Instead, the estimated energy for the lowest-lying such configuration of 2.54 ± 0.37 eV[26] is consistent with the present results.

Acknowledgment. This work was supported by the Division of Chemical Sciences, Geosciences, and Biosciences, U.S. Department of Energy, under contract DE-AC05-00OR22725 with Oak Ridge National Laboratory (ORNL), managed and operated by UT-Battelle, LLC. The ^{248}Cm, ^{249}Bk, ^{249}Cf, and ^{253}Es used in this work were supplied by the U.S. Department of Energy through the transplutonium element production facilities at ORNL.

OM049387V